

Biological Gain Control for High Dynamic Range Compression

Hedva Spitzer, Yan Karasik and Shmuel Einav

*Dept. of Biomedical Engineering, Faculty of Engineering, Tel-Aviv University
Tel-Aviv, Israel*

Abstract

The visual system has the ability to see and obtain detailed information from a highly dynamic range of a scene. For example, a person can observe items in one range by observing the inside of a dim room as well as outside through a window. An algorithm for high dynamic range compression that can be applied for still and video images is presented. This algorithm is based on a biological model that is also suggested for wide dynamic range and lightness constancy. It succeeded in automatically compressing the dynamic range of images to a 'human vision appearance' (as is commonly required in cameras and displays) while maintaining and even improving contrast. The biological basis is expressed as retinal mechanisms of adaptation (gain control), both 'local', and 'remote', that enable also video image applications by taking into account the dynamics of human adaptation mechanisms. The results indicate the significant and robust contribution of adaptation mechanisms in image appearance, and have been found appropriate for next generation High dynamic range cameras (CMOS based).

1. Introduction

The visual system has the ability to see and get detailed information from high dynamic range scenes. For example, a person can observe items in one sight while observing a dim room and outside through a window. An algorithm for high dynamic range compression that can be applied for still and video images is presented. This algorithm is based on a biological model which is suggested also for wide dynamic range and lightness constancy. It succeeds in automatically compressing the dynamic range of images to a 'human vision appearance' (as is commonly required in cameras and displays) while maintaining contrast and even improving it. The biological basis is retinal mechanisms of adaptation (gain control): 'local', and 'remote'. These mechanisms enable video image applications, since they take into account the dynamics of human adaptation mechanisms. The results indicate that the contribution of adaptation mechanisms to image appearance is significant, robust, and was proved to fit next generation High dynamic range cameras (CMOS based).

The common formats for the acquisition and display of images are usually based on 8 bit 3 color channels (R-G-B). Thus the dynamic range of intensity of the picture is 2 orders of magnitude. Natural light has 12 orders of magnitude, a single natural scene has 4 and a single sharp edge in a natural scene can reach 2 orders of magnitude. The human visual system can cope with 14 orders of magnitude.

Images obtained with standard film or digital cameras experience a loss in the clarity of details and colors at extreme light intensities, within shadows or/and from surfaces close to the light source. In recent years, more and more imaging devices are able to acquire high dynamic range views by more than 2 orders of magnitude, such as CMOS sensors for digital cameras, CT scanners, imaging systems for space research, etc. Software solutions are also capable of fusing multiple exposures of the same scene at a low dynamic range (in conventional format, 2 orders of magnitude) into one high dynamic range image (of approximately 4-5 orders of magnitude). Several current algorithms can deal with a large range image, acquired in one or several exposures, and convert it to a conventional display in one algorithm process, without the need to process the image at several stages or processing each exposure, separately.¹⁻⁴

High Dynamic Range Compression (HDRC) is also a psychophysical phenomenon in which a system is partly able to deal with a wide range of illuminations in the same scene. It is commonly assumed in the field that the visual system adapts to a wide range of intensities, and that this is performed through adaptive gain control mechanisms. The issue of a high dynamic range has not attracted much attention in the computational aspects of visual research,^{3,5-7} while it has recently been further described in the visual literature in the context of lightness perception and lightness constancy.^{8,9}

Previous studies on wide dynamic range using the computational approach can be classified into two broad groups, global and spatially variant operators (see reviews in: Refs. [2 and 5] are often Gaussian with different scales. In the next stage each scale is divided pointwise by its lower resolution image and thus obtain local image contrast. The last stage would be a compressive or attenuation function to each of the contrast images. The display image is calculated by multiplication or summation of the compressed images together. Note that

many of these studies used the log domain of luminance and actually made the calculation on the luminance channel. The issue of a high dynamic range was also related to that of color constancy.⁶

A few previous papers on the wide dynamic range compression have made cursory reference to the visual system. These include the work of Jobson and his colleagues, who developed a multiscale version of the Land's Retinex model for presenting a model for color constancy,⁶ aimed to be presented also as a dynamic range compression.^{6,10} Since they perform their algorithm on the RGB scale, they actually also calculated lightness constancy performance, which is revealed as dynamic range compression. In their model there is no reference to visual mechanisms, such as color coded receptive fields and physiological adaptation mechanisms. An additional algorithm inspired by the visual system is suggested by Pattanaik et al.^{3,11} The image is decomposed into multiscale resolution representations. The adaptation occurs using physiological threshold vs. intensity curves (Fig. 1 in Ref. [3]). In another study, an interactive tone mapping algorithm proposed also a simple model of visual adaptation.⁷

It has recently been suggested that the compression of high dynamic range without “haloes” can be obtained by removing pixels whose intensity variation is above a factor of 5.¹² We made a variation of their application in our algorithm in order to avoid the “halo” artifacts.

The approach we present here is based mainly on mechanisms of retinal biological local gain control¹³⁻¹⁵ and retinal receptive fields. The algorithm is also based on psychophysical findings such as the well known induction phenomenon, which shows that the perceived intensity (and color) of an image and a scene is not just a simple function of the spectral and intensity composition, but also depends on the spatial distribution of other stimuli in the field of view.

2. Model

The model is presented in two main stages. The first stage describes the transformation of visual stimuli to responses in retinal opponent cells. The second stage describes the adaptation mechanism, which includes the local and remote effects. Figure 1 presents a block diagram of the algorithm which includes only those different stages, that were applied for the implementation of real still images. (The model includes description of transformation of physical stimulus to the cone response, while the actual algorithm is related to RGB images and their processing, Fig. 1).

2.1. Transformation of an Image Into Retinal Opponent Receptive Fields

The first stage in the the model describes how an image is processed through the achromatic retinal opponent cells and their adaptation mechanisms. Our model can be regarded both as a physiological model and an algorithm that was inspired by the physiological mechanisms. The intensity channel is fed by rods and

cones at a low and a high scale of huge range of intensities, respectively. The retinal ganglion cells, which are the last level of processing in the retina, have a center-surround opponent structure in their receptive field (RF). These cells respond positively (increase in spike rate) to a specific intensity input to the center of their RF, and negatively (decrease in spike rate) to an opponent intensity input to the surround region of the RF.

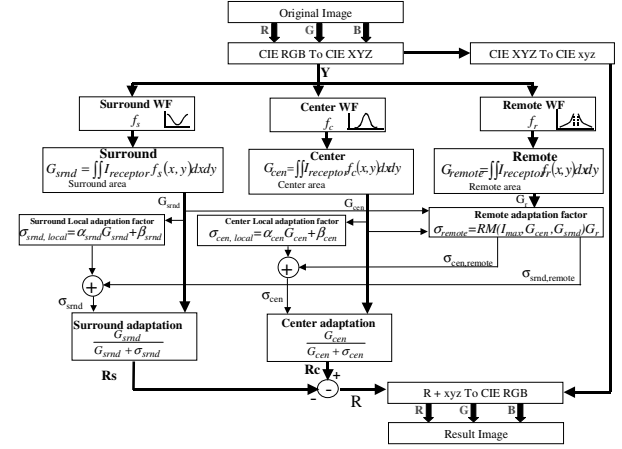


Figure 1. A schematic block diagram of the algorithm for compression of wide dynamic range. Components of the model are detailed in the text.

The input to the rods and cones level is the spectral composition of the light reaching the retina. The quantum catch is first expressed by an inner product of the spectral sensitivity with the reflectance properties of the surface at any specific location in the image, and with the spectral composition of the illumination falling on this location:

$$I_{\text{pigment}} = \int_{\text{visual range}} I(\lambda) \mathfrak{R}(\lambda) I(\lambda) d\lambda \quad (1)$$

where $I(\lambda)$ is the spectral absorption functions of the photoreceptors as a function of the wavelength λ ; $\mathfrak{R}(\lambda)$ is the reflectance function of the surface at any specific location in the image; and $I(\lambda)$ is the spectral composition of the illumination falling on this location.

The receptor responses of the pigments are then expressed by the Naka-Rushton saturation equation as a function of their input I_{pigment} .^{16,17}

$$I_{\text{receptor}} = \frac{I_{\text{pigment}}^n}{I_{\text{pigment}}^n + \sigma_{NR}^n} \quad (2)$$

The parameters n and σ_{NR} (the Naka-Rushton ‘semi-saturation constant’) were taken as constant parameter for all the pigments. Their photoreceptors’ responses I_{receptor} are normalized separately to a range of 0-1. (These two stages (Eq. 1 and 2) describe the physiological process in the visual system, but do not apply to the algorithm implementation where the image was already given in RGB scale.)

The spatial response profile of the ganglion cell's RF is expressed by a opponent Gaussians over the two sub-regions of the RF, 'center' and 'surround'. Contrary to what is common in the literature regarding the DOG (Difference of Gaussians) operation, in this model the subtraction operation is only performed after each sub-region is adapted.^{14,15} The 'Center' signal represents the central area of the RF of retinal ganglion cells, stimulating a single cone, as often occurs in the fovea.¹⁸ The 'center' signal was defined as an inner product of rod type (or cone) response, $I_{receptor}$ with its circular spatial profile f_c . This profile (Fig. 1) is a Gaussian decaying spatial-weight function (WF)¹⁵:

$$G_{cen} = \iint_{centerarea} I_{receptor} f_c(x, y) dx dy \quad (3)$$

where x and y represent the distance of the 'center' sub-region from the center.

The 'Surround' signal represents the surround sub-region of the RF of the retinal ganglion cell. The 'surround' signal, $I_{receptor}$, with the outer diameter of the annular 'surround' being three times larger than that of the 'center'¹¹:

$$G_{smd} = \iint_{surround\ area} I_{receptor} f_s(x, y) dx dy \quad (4)$$

where f_s is a Gaussian spatial weight function extending over the surround sub-region. The total weight of f_c is 1, whereas the total weight of f_s is 1/CSR (center:surround ratio of weights), which represents the weaker weight of the surround. CSR obtained a value of 1.5 or a similar value.¹⁴

For a description of the adaptation mechanism, a third signal, the 'Remote' signal, is required to represent the peripheral area that extends far beyond the borders of the classical RF of the ganglion cells. The inclusion of this signal is motivated by electrophysiological findings.^{19,20} The 'remote' area has the shape of an annulus, concentric to that of the 'center' and of the 'surround'. The inner diameter of the 'remote' is equal to the external diameter of the 'surround' and therefore does not overlap the 'center' or the 'surround'. The 'remote' signal, G_{remote} that feeds the opponent cells level is defined as the inner product of each receptor output with a remote spatial weight function f_r :

$$G_{remote} = \iint_{remotarea} I_{receptor} f_r(x, y) dx dy \quad (5)$$

where f_r is a Gaussian decaying spatial-weight function²⁰ over the remote area:

$$f_r(x, y) = \frac{\exp\left[-\sqrt{(x^2+y^2)} / K_{remote}\right]}{A_{remote}} \quad (6)$$

K_{remote} is a constant that defines the slope of the weight function and A_{remote} is a factor of normalization to a unit:

$$A_{remote} = \left(\iint_{remote\ area} \exp\left[-\frac{\sqrt{x^2+y^2}}{K_{remote}}\right] \right)^{-1} \quad (7)$$

2.2. Adaptation

The 'center' and 'surround' sub-regions adapt separately, with the adaptation values being based on electrophysiological findings.^{14,15} The response, R , of the on-center retinal cells, is therefore expressed by:

$$R(G, t) = \frac{G_{cen}(t)}{G_{cen}(t) + \sigma_{cen}(G_{cen}, t)} - \frac{G_{smd}(t)}{G_{smd}(t) + \sigma_{smd}(G_{smd}, t)} \quad (8)$$

where σ is the adaptation factor. σ is a function of $G(t')$ and time t , where $t' \leq t$.

A change in σ produces a gain control effect equivalent to the curve shift of the "response vs. log illumination" curve, which has been shown experimentally.¹³ The adaptation is reflected in a shift of the response curve as a function of time. Consequently, given that the change from the previous stimulation is sufficiently large, a curve shift will occur each time a new range of input intensities to a color channel is viewed, bringing the system to a new adaptation state. This curve shift causes an apparent decaying function of the response.

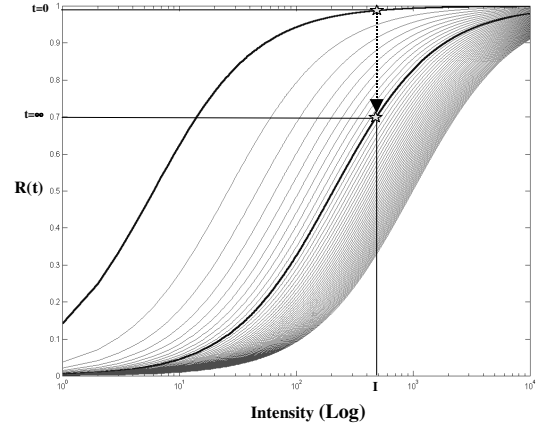


Figure 2. Illustration of the biological gain control, i.e., the curve-shifting mechanism which was applied as an adaptation mechanism. The curves display the response of each sub-region of a receptive field as a function of the luminance at this area at various adaptational levels. The dark left curve represents the curve response before the adaptation and right dark curve represents the response curve after the adaptation (see text).

Each of these adaptation factors, σ_{cen} and σ_{smd} , consist of 'local' and 'remote' components. The 'local' adaptation refers to adaptation occurring in the RF's sub-regions ('center' or 'surround') owing to their own inputs,

whereas ‘remote’ adaptation refers to the effect of regions peripheral to the ‘classical’ RF on its sub-regions.¹⁹⁻²²

The model was designed to comply with Weber’s law (which states that there is a constant proportion by which a standard stimulus must be increased in order to detect a response change), which has been found in relation to local adaptation.¹⁵ The model therefore suggests that the adaptation factors of each sub-region have separate ‘local’ and ‘remote’ components:

$$\begin{aligned} \sigma_{cen} &= \sigma_{cen,local} + \sigma_{L,cen,remote} \\ \text{where } \sigma_{cen,local} &= \alpha_{cen} G_{b_{cen}} + \beta_{cen} \\ \text{and } \sigma_{cen,remote} &= RM(I_{max}, G_{cen}, G_{srd}) G_{b_{remote}} \end{aligned} \quad (9)$$

while

$$RM(I_{max}, G_{cen}, G_{srd}) = c_{cen} \left(k(I_{max}) - |G_{cen} - mG_{srd}| \right) \quad (10)$$

The adaptation factors for surround sub-regions are similarly defined. α , β and c' are constants or c' is a function which is used as a modulation for the remote adaptation, σ_{remote} . $G_b(t)$ is the adapting component of the response of the RF sub-region. The description of the recursion function, G_b , its dependance on the history of the remote signal as well as its temporal parameter on the history stimulation is described in details in previous publication.^{22,23} The current study presents results only for still images. Therefore, we present only the specific case where the steady state condition is applied ($t=\infty$). In this case, $G_{b_{remote}}=G_{remote}$. Therefore, the response function is a substraction of the center response, R_c and the surround response, R_s , as following:

$$R(t=\infty) = R_{max} \left[\frac{d_c G_{cen}}{a_{cen} G_{cen} + b_{cen} + RM(I_{max}, G_{cen}, G_{srd}) G_{remote}} - \frac{d_s G_{srd}}{a_{srd} G_{srd} + b_{srd} + RM(I_{max}, G_{cen}, G_{srd}) G_{remote}} \right] \quad (11)$$

While k is function of I_{max} and R_{max} is a function the maximum value of intensity in (I_{max}) the image, and m is a constant ranging between 1-5, and while $a=\alpha+1$ and $b=\beta$. The parameters d_c and d_s present the weight function of the center and surround components. The degree of remote adaptation is controlled by the ‘ c ’ parameters: c_{cen} and c_{srd} for the remote adaptation of the ‘center’ and the ‘surround’, respectively.

3. Methods

3.1 Simulations

One of the common formats for digital storage of high dynamic range images is RGBE, which is used by the Radiance Rendering System to create the so-called Radiance Maps (Berkley University site). Four bytes are used in the RGBE format (instead of 3 in the conventional images) to create a representation similar to a floating point. The first 3 bytes represent the color channels (R-G-B) whereas the fourth byte represents the exponent (E), which is common to the three color channels.

Simulations were performed on real images by applying the above model on the luminance channel after extracting it from the chromatic channels. This was performed by transforming each pixel in the RGB image to the CIE XYZ scale, while extracting the Y values (the luminance values) and then transforming the scale to CIE xyz in order to store and retrieve the chromatic information of each pixel after the algorithm calculations on the luminance domain. The method described here can be applied mainly for images acquired by a digital camera, by different sensor methods. The application of above model and the calculations of center of a receptive field is related practically to each pixel in the image, such that the inner multiplication equations implemented as convolutions in the algorithm.

4. Results

4.1. Results of the Algorithm on Conventional Images

We examined a variety of conventional real images with our algorithm (with a standard display of 256 levels of luminance), using the same set of parameters. Our algorithm yielded satisfactory results in less than a few seconds in all cases, while we did not attempt to optimize the algorithm so that it would be more effective.

Figure 3 presents three different real images (left column) which are the original images that were taken (with permission) from the site of the ‘Trusight Enhanced Video Compression’ company.

4.2. Results of the Algorithm on HDR Images

Application of the algorithm to real life images, as specified in the Methods section, yielded a set of corrected images. The dynamic range in these images exceeded 30,000:1. The algorithm performance of this type of images was examined on almost the same set of parameters. However, it was different from the one used for the conventional images. As can be seen from the original image, it loses visibility around and within the bright light and much of the texture details are not visible in the dark areas. All these details are clearly visible in the corrected image.

5. Discussion

This study presents an algorithm based on a human vision model that succeeds in performing automatic wide dynamic range. It requires no *a priori* knowledge of illuminations or surfaces, and hence is fully automatic, while still enabling different degrees of correction through the algorithm’s parameters. Results of employing the algorithm for image compression demonstrate a significant compression while preserving, and even enhancing, the details in the image in the bright and dark zones.

5.1. Considerations for the Algorithm

The model is based on local and remote dynamic adaptation mechanisms, which cause the ‘curve-shifting’ effect.¹³⁻¹⁵ Since the human capability for wide dynamic

range is large, we assumed that the visual system performs this ability under both Scotopic and Photopic conditions in the same scene. Therefore, the Parvo as well as the Magno system, i.e., the color-coded cells in the retina and the achromatic coded cells in the retina, contribute to this ability. Both types of adaptation, local and remote, cause a change in cell response with time, reflecting the cell's transient response as a result of the curve-shifting effect.¹³⁻¹⁵ The transformation of cell receptive field regions to image pixels (see Methods) and cell transient responses to image correction dynamics, enabled application of the algorithm to the compression of still and video images.

The model suggests that the subtraction operation between the two color opponent RF sub-regions (Difference of Gaussians - DOG) is performed after the adaptation. The separate adaptation of two RF sub-regions has a computational advantage in that it makes the compression more cost-effective. When adaptation is carried out first and subtraction afterwards, the responses to the two surfaces drop to different points on the new adaptation curves where the slopes are higher and can yield larger differences in responses for the edges, after the center surround subtraction.

5.2. Comparison with Other Models

Several algorithms, which are multi resolution representations and contain the property of preserving local intensity ratios, have been used for dynamic range compression.^{1,2,4,12,24} These algorithms share several common features. They apply multiple lowpass filters (usually Gaussian filters). Each mean area in the image is then divided by its lower resolution image. Thus, they obtain the local contrasts. Next, a compressive function and its reconstruction function are applied.⁵ Although our algorithm is derived using a different approach (the biological motivation), our algorithm has some features in common with these general features, such as obtaining local contrast. However, even this feature is performed differently in our algorithm, since the adaptation is performed before the subtraction of the Gaussians of the 'center' and surround sub-regions of the receptive field. This type of adaptation operation and its stage of implementation in the model is different from previous visual motivated HDR model.³ Furthermore, our algorithm performs a remote adaptation operation (gain control, through modulated "curve-shifting") in addition to the local adaptation to each RF sub-region. Jobson and his colleagues,⁶ suggested that in general, Land's work on color constancy provides a good method for dynamic range compression (but not wide dynamic range) and color rendition.

In Land's later model^{25,26} he used neurophysiological building blocks which contained masks of center/surround spatially opponent operations, but did not include the physiological color-coded receptive fields, which we applied previously in our color constancy and contrast models.^{22,23} Jobson and his colleagues⁶ obtained color and lightness constancy to some extent, since their calculations were performed on the RGB scale. Spitzer and Semo color constancy algorithm²² did not focus on nor perform

lightness constancy a, but rather concentrated on visual physiology believed to not be performed by the same mechanisms in the visual system. For example, in order to process the dark regions in the image, the scotopic system (rods) has to be mobilized, while the photopic system (cones) must be mobilized to process the regions with extreme luminance. In our current model we processed only the intensity domain to perform the wide dynamic range, while preserving the original color of each pixel during the processing, returning these values after the calculations. Beyond the need to have two separate models for wide dynamic range and color constancy from the visual aspects (see above), we would like to emphasize the additional need from computational point of view, mainly due to the different ranges of luminance and color intensities for these two algorithms. In addition to the different approaches and goals of the two algorithms, different building blocks are used in their algorithm and in our two algorithms (the color constancy and wide dynamic range). We used color-coded receptive fields,^{22,23} and the mechanism of adaptation was applied separately to each receptive field region (center and surround). We also added a modulation component to the weight function of the remote adaptation (Eq. 10).

In summary, our algorithm²⁸ successfully performs good quality and wide dynamic range compression and is based on physiological mechanisms. The quality issue should be judged quantitatively in the future. However, the methods for this still need to be developed.

6. Conclusions

The automatic wide dynamic range compression algorithm has been demonstrated for a large amount of images and obtained with high contrast where the details in the image can be distinguished. The algorithm is based on human-vision and was motivated by a physiological model suggested for the early stages in the visual system. The algorithm includes dynamic gain control ("curve shifting") mechanisms which enable application for both still and video images. Its application to video images is performed by dynamically adjusting the algorithm's parameters at each frame according to the spectral content of the current frame as well as previous frames. A large repertoire of photographed images was tested. The algorithm performs wide dynamic compression in these images quite successfully.

7. Acknowledgement

This research was supported partly by the Ministry of Science and Industry, Israel.

8. References

1. J. Tumblin, and G E. Turk, "LCIS: A boundary for detail-preserving contrast reduction," in *Proceeding AMC SIGGRAPH 99A Annual Conference on Computer Graphics*, pg. 83-90. (1999).

2. R. Fattal, D. Lishinski, and M. Werman, "Gradient domain high dynamic range compression," *ACM Transactions on Graphics, in Proceeding. ACM SIGGRAPH*. (2002).
3. S.N. Pattanaik, J. A. Ferwerda, M. D. Fairchild, D. P. Greenberg "A Multiscale Model of Adaptation and Spatial Vision for Realistic Image Display," *Proceedings SIGGRAPH 98*, pg.287-298. (1998).
4. F. Durand and J. Dorsey, "Fast Bilateral filtering for the display of high dynamic range images," *ACM Transactions on Graphics*, ACM, 21, pg. 257-266. (2002).
5. J. M. DiCarlo and B. A. Wandell, "Rendering high dynamic range images," *In Proceeding of the SPIE: Image Sensious*, 3965, pg. 392-401. (2001).
6. D. J Jobson, Z. Rahman and G.A. Woodel, "A multiscale retinex for bridging the gap between color images and the human observation of scenes," *Image Processing 6*, IEEE Trans, pg. 965-976. (1997). F. Durand and J. Dorsey, "Interactive tone mapping," *Proceedings of the Eurographics Workshop. Rendering Techniques 2000*. Springer verlag, pg. 219-232, (2000).
7. Z. Rahman, D, J. Jobson, and G. A. Woodel, "A multiscale retinex for color rendition and dynamic range compression," *International Symposium on Optical Science, Engineering, and Instrumentation*, SPIE. (1996).
8. E. Adelson, "Lightness perception and lightness illusions," *In the new cognitive neurosciences, 2nd ed., M. Gazzania ed. Cambridge, MA: MIT press*, pg. 339-251, (2000).
9. E. H. Land, "Recent Advances in Retinex Theory," *Vision Res*, 26, pg. 7-21. (1986).
10. S. N. Pattanaik, J. E. Tumblin, H. Yee, and D. P. Greenberg "Time-Dependent Visual Adaptation For Fast Realistic Image Display," *Computer Graphic Proceedings, ACM SIGGRAPH 2000*, pg. 7-54. (2000).
11. S. Pattanaik and H. Yee, " Adaptive gain control for high dynamic range image display," *10 SCCG 2002*. (2002).
12. B. Sakmann and O.D. Creutzfeldt, "Scotopic and mesopic light adaptation in the cat's retina," *Plugers Arch*. 313, pg. 168-185. (1969).
13. R. Shapley and C. Enroth-Cugell, "Visual Adaptation and Retinal Gain Controls," *Progress in retinal Res*. 3, pg. 263-346. (1984).
14. R. Dahari and H. Spitzer, "Spatio-temporal adaptation model for retinal ganglion cells," *J. Opt. Soc. Am A* 13, pg. 419-439. (1996).
15. K. I.Naka and W. A. H. Rushton, "S-Potentials from color units in the retina of fish," *J. Physiol*. 185, pg. 536-555. (1966).
16. R. A. Normann, I. Perlman and , P. E. Hallet, "Cone Photoreceptor Physiology and Cone Contribution to Color Vision," in *Gouras, P. (editor), The Perception of Color*, pg. 146-162, MacMillen Press, London. (1991).
17. B. B. Lee, "Receptive field structure in the primate retina," *Minireview. Vision Res*. 36, pg. 631-44. (1996).
18. A.Valberg, B.B Lee., B.B. O.D Tigwell, and A Creutzfeldt, "simultaneous contrast effect of steady remote surrounds on responses of cells in macaque geniculate nucleus," *Exp. brain res*. 58, pg. 604-608. (1985).
19. O. D.Creutzfeldt, J. M. Crook Kastner, S. Chao-Yi Li and Xing Pei, "The neurophysiological correlates of color and brightness contrast in lateral geniculate neurons: I. Population Analysis," *Exp. Brain Res*. 87, , pg. 3-21. (1991).
20. A. Tsofe, G. Rotgold and H. Spitzer, "Remote adaptation effect on perceived subjective color: A model approach," *Color Research & application*. (2003), in press.
21. H. Spitzer and S. Semo, "A biological color constancy model and its application for real images, " *Pattern recognition*, 35, pg. 1645-1659. (2002).
22. H. Spitzer and E. Sherman, "Color Contrast: A Biological Model and its Application for Real Images, " *Proceeding in: Color in graphics, imaging and vision*, CGIV 2003. (2003)
23. E. Reinhard, M.stark, P. Shirley and J. Ferwerda, "Photographic tone reproduction for digital images," *Proceedings SIGGRAPH 2002*, pg. 267-276. (2002).
24. E. H. Land and J. J. McCann, "Lightness and the Retinex, " *Theory, J. Opt. Soc. Am A* 61, pg. 1-11. (1971).
25. E. Land, "An alternative technique for the computation of the designator in the retinex theory of color vision, " *Proc Nat. Sci.*, 83, pg. 3078-3080. (1986).
26. H. Spitzer and A. Rosenbluth, "Color constancy: the role of low-level mechanisms," *Spatial vision*, 15, pg. 277-302. (2002).
27. H. Spitzer and Y. Karasik, "Method of and device for compressing a dynamic range of still and video images," US Patent pending. (2003).

9. Biographies

Hedva Spitzer received her B.A. degree from the Hebrew University in Jerusalem, and M.A. and Ph.D. in Electrophysiology from the Hebrew University. She directs the Vision Research Lab in Biomedical Engineering department in Engineering faculty at Tel Aviv University. Her research interest in the recent years are concentrated on color and adaptation mechanisms with applications also to technology.

Yan Karasik received his B.Sc. in Electrical Engineering from the Technion - Israel Institute of Technology. He is currently completing his M.Sc. in Biomedical Engineering department Tel-Aviv University and his thesis is performed in Vision Research Lab in Biomedical Engineering Department on the subject of wide dynamic range compression.

Shmuel Einav Professor of Biomedical Engineering at Tel Aviv University, was born in Israel. Received his B.Sc. in Mechanical Engineering and M.Sc. in Nuclear Engineering at the Technion, Israel, and Ph.D. degree in Mechanics and Physiology at SUNY at Stony Brook. He was the founding Chairman of the Department of Biomedical Engineering at Tel Aviv University. His main research interests are in Hemodynamics, the cardiovascular system and blood-tissue interaction.



Figure 3. Demonstration of the algorithm performance on an image of standard format (left) while the original image is also presented (right).

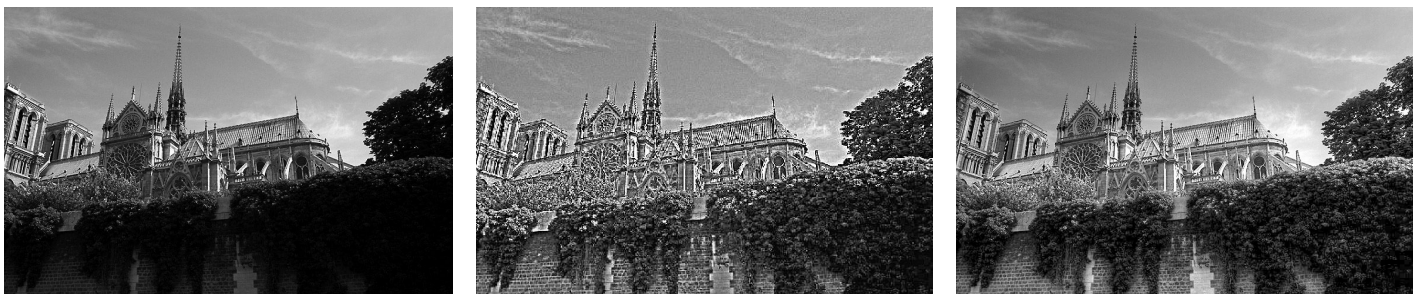


Figure 4. Additional two examples of algorithm performance on standard format are presented, with comparison to those of Fattal et. al.,² (right column). It can be seen that our method produced better exposure -of the details in the dark zones in the images and better enhanced contrast (middle column) than those of Fattal et al.

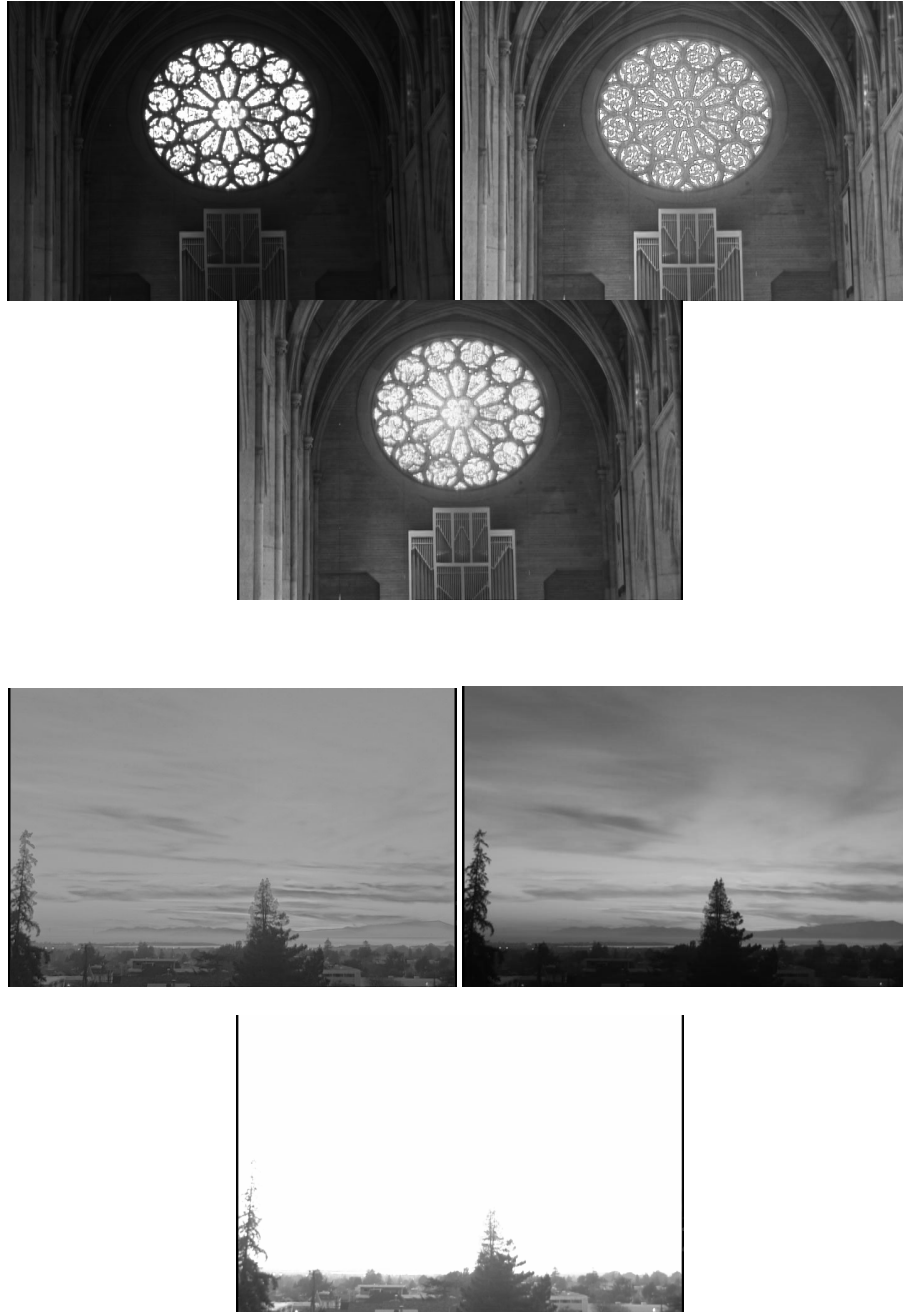


Figure 5. The figures demonstrate the algorithm performance (middle column) of compression of two HDR images (left column) which are compared with the performance of a recent study²⁴ of compression of wide dynamic range (right column). It can be seen that the details in the bright zones are exposed in the sky as well as the dark zones, middle column, and also in the light zones, better than in the compressed image done by Reinhard et al.²⁴



Figure 6. The HDR Cathedral image (left) was compressed by several groups, and the best printed performance until now, as far as we know, demonstrated by Fattal et al (right). Our algorithm (middle) succeeded to better expose details mainly in the bright zones (middle) Note that the vitrage in the right window and the top dome in the middle are exposed in comparison to this details in the right.²